

# The influence of galaxy mergers on the mass dispersion of brightest cluster galaxies

Th. Jagemann<sup>1</sup>

*Astronomisches Rechen-Institut Heidelberg,  
Mönchhofstraße 12-14, D-69120 Heidelberg, Germany*

thomas.jagemann@esa.int

## ABSTRACT

The absolute magnitude of the brightest galaxy of clusters varies remarkably little and is nearly independent of all other physical properties of the cluster as, e.g., its spatial extension or its richness. The question arises whether the observed small scatter is compatible with the assumption of dynamical evolution of the cluster. This is investigated with the help of statistical analysis of the results of cluster simulation. The underlying interaction process is merging (and also destruction) of smaller galaxies forming the giant galaxy. The cluster itself is supposed to be in virial equilibrium.

We find that the evolutionary importance of merger processes grows with decreasing scale. Rich clusters as well as their brightest members evolve merely slowly whereas compact groups as well as their brightest members evolve more rapidly and more violently. We also find that the number of merger processes leading to the growth of the brightest cluster galaxy (BCG) is small enough to keep the BCG mass dispersion below the measured value. Our simulation substantiate that just the combination of the initial distribution function and the following merging to form the BCG can explain the remarkably small variance of mean BCG masses between clusters of different size and different number of galaxies.

*Subject headings:* Galaxies: clusters: general – Galaxies: evolution – Galaxies: interactions – Galaxies: mass function

---

<sup>1</sup>Current address: ESA/ESTEC, Postbus 299, 2200 AG Noordwijk, The Netherlands

## 1. Introduction

The mean absolute magnitude of brightest cluster galaxies is  $\langle M_{\text{VI}} \rangle = -22.7$  mag with a dispersion of  $\sigma(M_{\text{VI}}) = 0.4$  mag (Hoessel, Gunn, & Thuan (1980)). The distribution of BCG absolute magnitudes is well represented by a Gaussian distribution (e.g. Postman & Lauer (1995)), and the relative variation of luminosities yields

$$\frac{\sigma(L)}{L} = 0.5. \quad (1)$$

Batcheldor et al. (2007) show that the luminosity dispersion in the near infrared is even less. Due to this small intrinsic dispersion BCGs are ideal tools for cosmological distance determination (Sandage (1972); Postman & Lauer (1995)). Furthermore their theoretical investigation offers the possibility to understand the properties and evolution of the cluster itself and its members.

Sandage (1972) points out that there is a variety of possible accounts for the observed scatter in BCG apparent magnitudes, but all contributions but intrinsic dispersion (i.e. scatter in absolute magnitude) seem to remain small, in particular is there no systematic trend with redshift. At least the small total dispersion shows that any single dispersion contribution remains small.

There are many kinds of suggestions trying to explain the observed small scatter in magnitudes of brightest cluster galaxies. One possibility is the existence of a common luminosity function all galaxies of a cluster (including the brightest one) are drawn from (Schechter & Peebles (1976)), either with or without further development. The alternative consists of a unique creation process, a “standard mold”, or a not yet discovered physical effect that delimits the luminosities of galaxies and cuts off the bright end of the luminosity function. This hypothesis is underpinned by the astonishing fact that brightest galaxies of rich clusters are just as luminous as the brightest observed field galaxies (Humason, Mayall, & Sandage (1956)).

How special are BCGs? It has been argued that surface brightness profiles of BCGs are well fit by the same Sérsic law that describes less-luminous spheroids and obey the same relations between fitting parameters that characterise E/S0 galaxies generally (Batcheldor et al. (2007)). On the other hand, v.d.Linden et al. (2007) show that BCGs contain a larger fraction of dark matter as compared to non-BCGs of the same stellar mass, influenced by the cluster environment.

X-ray observations of the intracluster medium (e.g., Peres et al. (1998)), in particular of the cluster core, has given rise to the assumption of cooling flows depositing up to  $100 M_{\odot} \text{ yr}^{-1}$ , building up the BCG over many Gyrs. However, Motl et al. (2004) support the alter-

native that cores of cool gas are being built from the accretion of discrete stable subclusters. At the same time they realise that the common presence of substructure in galaxy clusters argues for accretion or merger events that occurred sufficiently recently not to be erased by relaxation of the cluster ( Bird (1994)).

Galactic cannibalism, i.e. the accretion of the existing galaxy population through dynamical friction and tidal stripping predominantly in the evolved cluster, has been proposed by several authors (e.g., Ostriker & Hausman (1977)). Further investigations by Merritt (Merritt (1983), Merritt (1984), Merritt (1985)) and others (e.g., Lauer (1985), Dubinski (1998)) showed, however, that galaxies are moving too fast and are significantly tidally truncated thereby suppressing dynamical friction. They concluded that the dynamical friction timescales are generally too long such that galaxies could therefore only accrete a small fraction of their total luminosity within a Hubble time.

Galactic mergers remain as the most likely dynamical effect that dominates BCG evolution. But given a vivid merger history, it is problematical how a uniform magnitude of the brightest cluster galaxy can get over frequent encounters while being exposed to mergers with other galaxies, or deletion. Tightly related to this puzzle, the question comes up whether the common luminosity function of all up to date analysed clusters is a direct consequence of the initial mass fluctuations of the early universe – or otherwise, if the mass spectrum at that time was an entirely other one, and evolution processes provide for the universality of the luminosity function.

However, the scenario seems less agitated. Hoessel (1980) estimates, correlating spatial extension and luminosity of BCGs, that mergers of galaxies of comparable size lead to the formation of the first-ranked member. As he divides the collapse time of a cluster by the time that pass between two close encounters of two relatively big galaxies, he obtains about four merger events forming the BCG. This result coincides with the number of observed cores in cD-galaxies. In the same way, the luminosity function changed only little, because merger processes operate effectively only on large massive galaxies (Trèvese, Cirimele, & Appodia (1996)).

Numerical simulations of large groups of 50-100 spherical galaxies in an equilibrium cluster have been done by Funato, Makino, & Ebisuzaki (1993), Bode et al. (1994), Garijo, Athanassoula, & Ga (1997). These simulations find a runaway merging process occurring near the cluster center forming a BCG. Recent analyses of the Millenium Simulation (Springel et al. (2005)) by Lucia et al. (2006) indicate that, on the one hand, the most massive elliptical galaxies have the oldest and most metal rich stellar populations. On the other hand, massive ellipticals are predicted to be assembled later than their lower mass counterparts, and they have a larger effective number of progenitor systems (reaching up to  $N_{\text{eff}} \approx 5$ ).

In order to investigate the influence of galaxy mergers on the BCG mass dispersion systematically and with statistical significance, we set up ensembles of Monte Carlo simulations of cluster evolution. A set of parameters that describe the initial conditions of the cluster is defined, then the cluster evolution is simulated and the evolved cluster is characterized. After that, the simulation is repeated from the beginning with the same initial parameter set, evolving to a different cluster due to the somewhat stochastic nature of galaxy encounters. The number of simulations of cluster evolution for a fixed set of initial conditions defines the ensemble size, which in turn determines the level of confidence with which parameters of the evolved cluster can be specified. Then one of the initial cluster parameters is varied leaving all other parameters fixed, and an ensemble of cluster simulations is run in the same way as described above. This parameter variation is repeated with a certain step size within an interval given by observations. The interval is supposed to cover all occurrences in nature (e.g., the cluster richness) and/or uncertainties as the true value could not yet be fixed by observations (e.g., the fraction of cluster mass that is still bound to individual galaxies, Springel et al. (2001)). Having gone through all steps of the variation of this particular cluster parameter, the next parameter is varied leaving all others fixed. In this way, the full parameter space is covered, while all parameters are varied independently of each other. Possible correlations of initial cluster parameters (e.g., size and richness) can easily be applied afterwards by restricting the parameter space to a subspace. The required computing power for such a large number of repeated simulations of cluster evolution over a Hubble time, covering a broad parameter space, is still beyond the capacities of present-day detailed N-body simulations. That is why a Monte Carlo code has been developed to investigate the small BCG mass dispersion, surpassing a purely analytical description (e.g., Merritt (1983)) with the power of simulating statistically significant ensemble sizes.

The structure of this paper is as follows: In the next section the simulation method is described. Section 3 details the parameter set and the mass dispersion. Section 4 presents the results of three simulation sets with exemplarily representative parameter sets. A discussion of the results is given in Section 5. Finally, Section 6 briefs the conclusions of this work.

## 2. The model

Numerical simulations require the masses of the galaxies. On the presumption of a given mass-to-light ratio  $\Upsilon$ , Eq. (1) is directly translatable into the BCG mass dispersion. Though masses resulting from dynamical simulations are still dependent on  $\Upsilon$  once compared with the observed luminosities, the relative variation does not depend on  $\Upsilon$ .

The following subsections briefly describe the model assumptions that enter the simu-

lation computations. For further details see Jagemann (1997).

## 2.1. The cluster

The cluster simulation starts with  $N$  galaxies homogeneously distributed in a sphere of radius  $R$  and total mass  $M$ .  $R$  and  $M$  are kept constant in time in the course of development; in other words, we assume that the cluster is isolated and decoupled from the Hubble flow. At the beginning the number of galaxies in the cluster equals  $N = N_0$ .  $N$  diminishes in the course of time due to mergers and destruction of galaxies. The mass of the destroyed galaxies is counted to the intergalactic medium, so that the total mass of the cluster remains constant.

The galaxy masses are initially drawn from the exponential distribution function discussed in Sect. 3. The model starts from the assumption that the total mass of the galaxy cluster is proportional to the total mass of all galaxies:

$$M_{\text{tot}} = N_0 M_0 \cdot k \tag{2}$$

Here  $N_0$  is the initial galaxy number and  $M_0$  is the mean galaxy mass (Sect. 3). Then the constant  $k$  is the ratio of cluster mass to galaxy mass, i.e. the ratio of mass-to-light ratio of the cluster (in the following denoted by  $\Upsilon_{\text{cluster}}$ ) and mass-to-light ratio of the galaxies:

$$k = \frac{\Upsilon_{\text{cluster}}}{\Upsilon_{\text{galaxies}}} \tag{3}$$

The total mass of a (rich) cluster is of the order of  $10^{15} M_{\odot}$ . Therefore the mass-to-light ratio of a cluster is within the range  $[200; 500] \Upsilon_{\odot}$ , and so the discrepancy between the mass-to-light ratios of present clusters as a whole and their individual members is at least  $k = 5$  and probably more. An interesting and crucial question concerning the interaction between galaxies of a cluster is how much of the cluster dark matter is really gravitationally bound within galaxies (Merritt (1985)), i.e. the value of  $k$ . Two possible extreme cases are imaginable: either the dark matter hides within individual halos of single galaxies, or these halos are smeared over the whole intergalactic background due to tidal processes or similar effects. As virial velocities of the galaxies are determined by the total cluster mass, whereas individual galaxy masses enter decisively those equations that determine the interaction between two encountering galaxies, the trend resulting from the different extreme cases can be anticipated:

If dark matter exists in individual halos, the merger cross section is much larger than in a cluster containing significantly intergalactic matter, so the model develops more rapidly and more violently. This work considers these two cases.

## 2.2. The galaxies

In this paper individual galaxies are described by two parameters: their radius  $r_i$  and their mass  $M_i$  ( $i = 1 \dots N$ ). Mass and radius are changing in the course of cluster evolution; at the beginning, the masses of cluster galaxies are characterized by a distribution function with characteristic mass  $M_0$  and an associated distribution function in galaxy radii with characteristic radius  $r_0$ .

The evaluation of galaxy encounters is done under the assumption that galaxies are represented by Plummer spheres:

$$\rho(r) = \frac{3}{4\pi} \frac{Ma^2}{(r^2 + a^2)^{5/2}} \quad (4)$$

Here  $a$  is the Plummer radius,  $M$  is the total mass of the galaxy and  $G$  is the gravitational constant. Later, for the energy transfer in the tidal approximation, the root mean square (RMS) radius of the extended perturbed mass distribution is needed. So we further assume a cut-off radius  $r_{\text{RMS}} \approx 4.3a$ . In the following, we call this proportional factor  $\beta := r_{\text{RMS}}/a$ . The galaxy radii  $r_i = r_{\text{RMS}}$  are related to the drawn masses via the Faber-Jackson-law. Calculating interaction of cluster galaxies, the significant parameter is not the radius but rather the binding energy which computes for a Plummer model to:

$$E = -\frac{3\pi}{64} \frac{GM^2}{a}. \quad (5)$$

## 2.3. Encounters

Encounters of galaxies let the model evolve. In this work, encounters are described by the two parameters  $v$  and  $B$ .  $v$  is the relative velocity, and the maximum impact parameter  $B$  defines the maximum separation between two passing galaxies that is evaluated to be an encounter. Fixing the total cluster mass  $M_{\text{tot}}$  and characteristic radius  $R$  to be independent model parameters, the mean square of the spatial velocity  $v_3^2$  is set by the virial theorem that is assumed to be applicable to the cluster:

$$v_3^2 = f^2 \frac{G M_0 k N}{R} \quad (6)$$

This procedure is in contradistinction to the procedure of Krivitsky & Kontorovich (1997). They find a kind of “explosive” merging without the additional constraint of virial equilibrium.

The radius  $R$  of the sphere is assumed to be proportional to the gravitational radius with proportionality factor  $f^2$ . In addition, we assume the spatial virial velocity  $v_3$  (that also determines the rate of encounters) equals  $\sqrt{\langle v^{-2} \rangle}$  that has to be put into the formula of energy transfer.

The impact parameter  $b$  of the actual encounter is chosen within the limits of  $[0; B]$  such that encounters are uniformly distributed upon the maximum encounter cross-section  $\pi B^2$ .

Using the impulse approximation, in this model  $B$  is defined the way that the error due to neglecting encounters with impact parameters greater than  $B$  is less than one per cent for a galaxy of standard size  $r_0$  ( $r_0$  corresponds to  $M_0$  via the Faber-Jackson-law).

The mean time between two encounters is given by

$$\Delta t = \frac{8R^3}{3vB^2} \frac{1}{N(N-1)} \quad (7)$$

and diminishes with decreasing galaxy number  $N$  during the cluster development. The total development time is set to  $T = 10^{10}$  yrs.

## 2.4. Development

Gravitational interaction is the origin of cluster development. We compare the kinetic energy from orbital motion of two encountering galaxies with their internal energies. The binding energy of an individual galaxy increases at the expense of the orbital energy, i.e. at the expense of the total kinetic energy of their relative motion. As long as the total energy transfer  $\Delta E_i + \Delta E_j$  is less than the kinetic energy of the relative motion, the pair of galaxies is assumed to stay unbound. The energy input leads to an increase in binding energy of a galaxy which therefore expands. If energy input exceeds the binding energy of the concerning galaxy, this leads to its destruction.

But if the total energy transfer is higher than their kinetic energy,

$$\Delta E_i + \Delta E_j > E_{\text{kin}}, \quad (8)$$

the encounter ends up in a bound system, and it is assumed that the galaxies merge. If the encounter leads to a merger event, both participating galaxies are replaced by a single one (the remnant), and its mass and radius has to be recalculated. The remnant mass is simply the sum of both galaxy masses, and the radius is computed from energy conservation:

$$E_{\text{R}} = E_i + E_j + E_{\text{kin}}. \quad (9)$$

It is possible that the remnant binding energy becomes  $E_{\text{R}} > 0$ , if

$$E_{\text{kin}} > -(E_i + E_j). \quad (10)$$

In this case no remnant is created and both galaxies break up.

To calculate energy exchange, the energy transfer is expressed using the impulse and tidal approximation (Spitzer (1958)) combined with a smooth interpolation of the two limiting cases of  $b = 0$  and  $b \geq \hat{b}$  ( $\hat{b} = 5 \max(r_{\text{h},i}, r_{\text{h},j})$ ,  $r_{\text{h}}$  is the median radius of the respective perturbed system).

The energy transfer of a particle of mass  $M_j$  passing an extended particle system at distance  $b$  with velocity  $v$  according to impulse and tidal approximation is

$$\Delta E_i = \frac{4G^2 M_j^2 M_i r_i^2}{3v^2 b^4}, \quad (11)$$

where  $r_i$  is the RMS-radius of the perturbed system  $i$  ( Spitzer (1958)).

In the case of central penetration ( $b = 0$ ) the energy transfer between two identical Plummer models is given by

$$\Delta E_{\text{max}} = \frac{G^2 \beta^2 m_j^2 m_i}{3v^2 r_i^2} \quad (12)$$

where  $\beta$  was introduced in Subsect. 2.2. The interpolation formula is then assumed to be

$$\frac{\Delta E}{\Delta E_{\text{max}}} = \frac{1}{1 + \frac{\beta^2}{4r_i^4} b^4} \quad (13)$$

(Fig. 1).

Proceeding this way we use two terms of energy transfer in high speed encounters, i.e. in encounters where relative velocities are higher than the galaxy internal velocity dispersion.



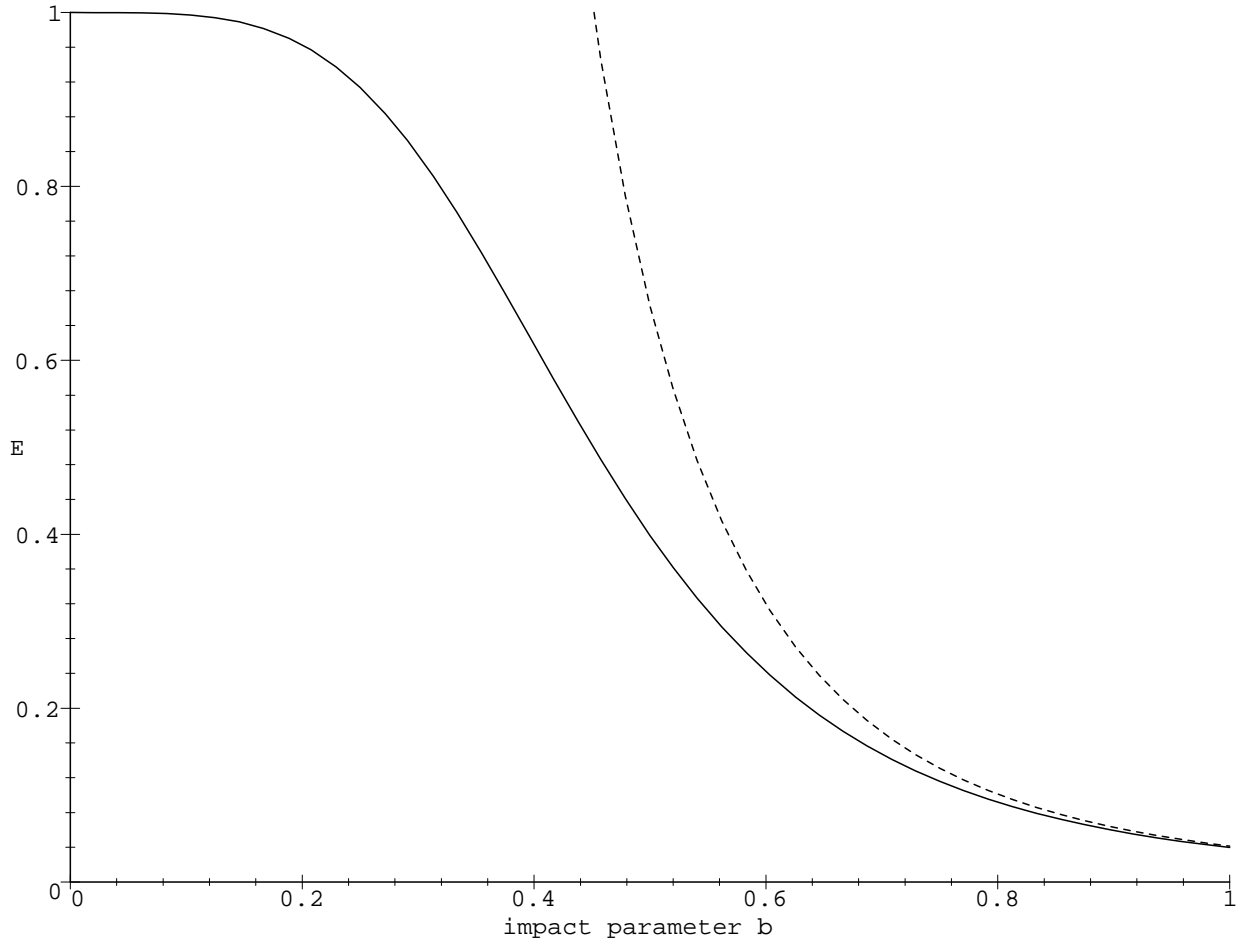


Fig. 1.— Energy transfer with interpolation formula Eq. 13. Abscissa:  $b/\hat{b}$ , ordinate:  $\Delta E/\Delta E_{\max}$ ; dashed line: impulse approximation, solid line: interpolation.

This approximation is not too crude (Aguilar & White (1985)) although galaxy relative velocities are about as high as their star velocities.

Other dynamical processes, especially dynamical friction between galaxies or galaxies and the intergalactic background, tidal interaction between galaxies and the cluster potential as well as mass-loss due to ram-pressure are neglected.

### 3. Mass dispersion

Trying to understand the BCG mass dispersion, it is necessary to know more about the stochastic variance, inherent in the distribution function. When drawing  $N$  galaxies from a given frequency distribution, there is already a dispersion in the mass of a distinct, e.g. the brightest, galaxy depending on the kind of distribution and the number of drawn galaxies. An analytical approximation of the global luminosity distribution of galaxies in today's clusters is Schechter's law (Schechter (1976)):

$$N(L) dL = N_* \left(\frac{L}{L_*}\right)^\alpha \exp\left(-\frac{L}{L_*}\right) \frac{dL}{L_*} \quad (14)$$

with

$$\begin{aligned} \alpha &= -5/4 \\ L_* &= 1.0 \cdot 10^{10} h^{-2} L_\odot \text{ in the visual band} \\ N_* &\in [20; 115]. \end{aligned}$$

$\alpha$  is given within an error of 20%, but there are also votes for an exponential distribution in compact clusters ( $\alpha = 0$ ) differing from that of field galaxies (Geller & Peebles (1976)). In any case, solely the number of the brightest (cD-) galaxies in the centres of galaxy clusters are not exactly accounted for (Dressler (1978), and references therein). This fact by itself is an indication of the answer to the central question: Is Schechter's law the result of development in kind of merger and destruction processes or does it reflect the mass spectrum in the early universe (Lauer (1985))? Since the BCG is in an exceptional position with respect to Schechter's law and does not fit the global distribution, it is not probable that Schechter's distribution accrues from a different distribution (except that other than development processes would affect the BCG luminosity). Otherwise the distribution would include the BCG.

With the assumption of a specific mass-to-light ratio of individual galaxies, galaxy masses can be drawn from a universal mass distribution. Because of better analytical han-

ding and to avoid divergences galaxy masses of the model cluster are drawn from an exponential distribution. In this case, the initial probability distribution is

$$p_{\text{BCG}}(M) dM \equiv N \left(1 - e^{-\frac{M}{M_0}}\right)^{N-1} \frac{1}{M_0} e^{-\frac{M}{M_0}} dM, \quad (15)$$

shown in Fig. 2.

In this case the expected value of the most massive initial galaxy can be written as an harmonic sum that depends on the mass  $M_0$  characterizing the distribution function and on the number of drawn galaxies  $N_0$ :

$$\langle M_{\text{BCG}} \rangle = M_0 \sum_{k=1}^N \frac{1}{k}. \quad (16)$$

The BCG mass dispersion is then computed to

$$\sigma_{\text{BCG}} = M_0 \sqrt{\sum_{k=1}^N \frac{1}{k^2}}. \quad (17)$$

With  $N = 1000$ , e.g., the relative deviation computes to  $\sigma_{\text{BCG}}/\langle M_{\text{BCG}} \rangle = 0.17$ . Though the expected value of the BCG masses increases with galaxy number, the relative deviation does not. Generally the fact is remarkable, that initially BCG masses depend on the number of galaxies, whereas in reality such a dependence is not found, and the BCG relative mass dispersion is distinctly smaller for all numbers of galaxies than the observed one. These differences may be due to development processes, although additional correlations among  $R$  and  $N$  may cause selection effects in  $(N, R)$ -space.

Statistical statements about clusters of galaxies are derived from model assumptions depending on several parameters. Thus the resulting quantities to be analysed are only estimates of the mean sampled over infinite runs. The accuracy, given as relative  $1\sigma$  variance, is proportional to the square root of the number of simulation runs. Differently set up model clusters with the same set of initial parameters are here called an ensemble. So since all our simulation results are based on ensemble sizes of 100 runs, they are accurate to within 10%.

Additionally, any dispersion in absolute magnitudes (or masses, respectively) in a model that depends on variable parameters will generally depend on these parameters, too. For example, BCG masses – as well as their dispersions – that are drawn from a distribution function depend on a characteristic mass  $M_0$  scaling this function and depend also on the total number of galaxies  $N_0$  drawn from this distribution.

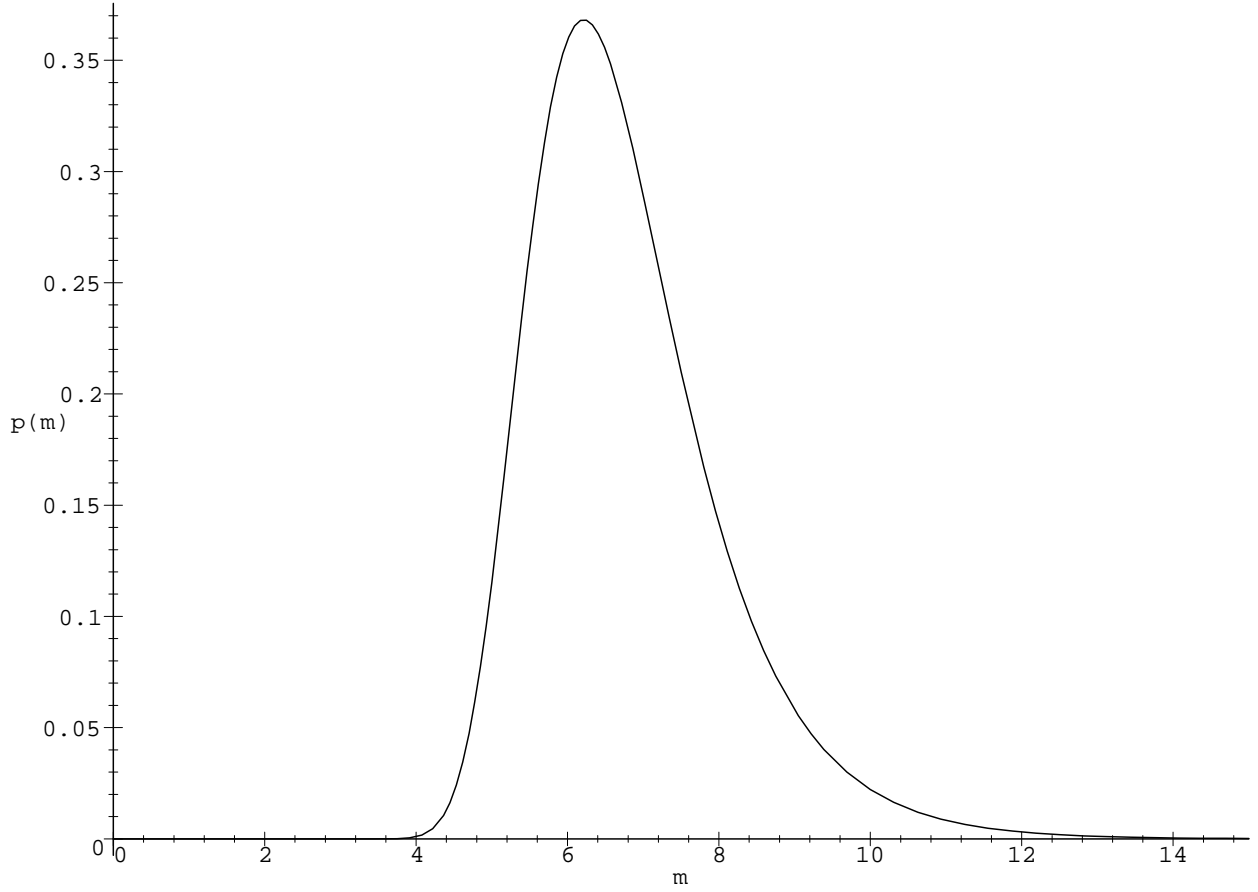


Fig. 2.— Frequency distribution of the brightest cluster galaxies with exponential mass distribution and  $N = 500$  and  $M_0 = 1$ .

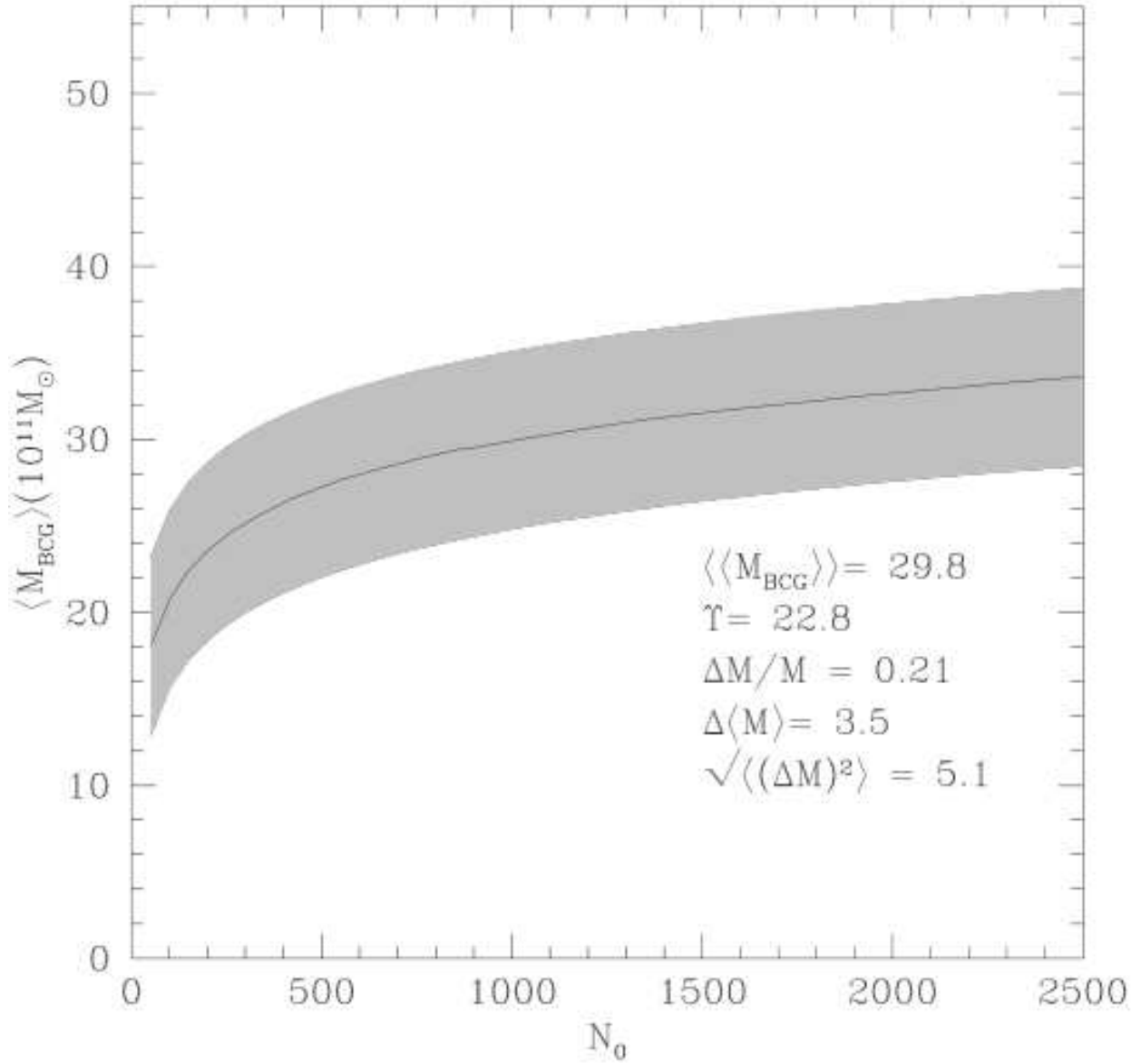


Fig. 3.— BCG masses and their variance at the beginning of the simulation. Initial parameters are:  $M_0 = 4 \cdot 10^{11} M_{\odot}$ ,  $r_0 = 15$  kpc,  $v_0 = 800$  km/s,  $R = 3$  Mpc,  $T = 10$  Gyr.

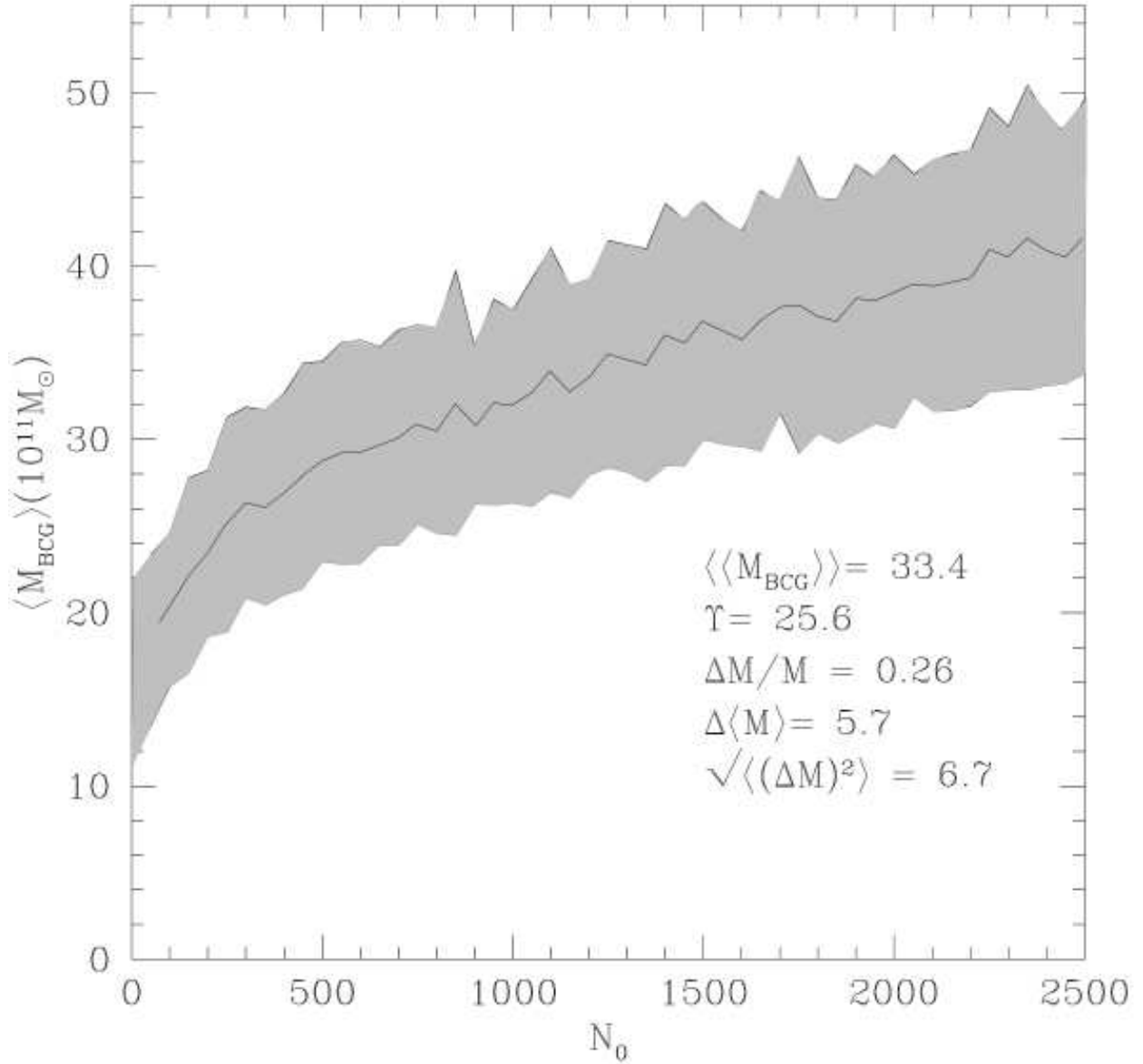


Fig. 4.— BCG masses and their variance at the end of the simulation. The initial parameters are the same as in Fig. 3.

Figures 3 and 4 illustrate the dependence of the mean of BCG masses on the initial number of galaxies. Likewise, standard deviations belonging to any value of  $N$  are shown, too. Figure 3 describes the initial state, Fig. 4 the evolved state. The curve in Fig. 3 is smooth, because the expected value of BCG mass and dispersion are theoretically computable. In Fig. 3 the stochastic 10% noise of the mean values is obvious.

In order to calculate the total dispersion of BCG masses, let these masses be a function of a vector  $\vec{x}$  in parameter space. Furthermore, assume that a distribution function  $p_{\vec{x}}(M)$  is given. The expected value of  $M$  then averages the ensemble and the parameter space to

$$\langle\langle M \rangle\rangle := \int_{\vec{x}} \langle M(\vec{x}) \rangle p(\vec{x}) d\vec{x}, \quad (18)$$

where  $\langle M(\vec{x}) \rangle$  means an ensemble average. The mass dispersion averages the ensemble and the parameter space to

$$(\Delta M)_{\text{tot}}^2 = \langle(\Delta M)^2\rangle + \langle\langle M \rangle\rangle^2 - \langle\langle M \rangle\rangle^2, \quad (19)$$

where the inner brackets always denote an ensemble average. Thus, the total dispersion is the expected value of the individual dispersion in  $\vec{x}$  plus the scatter of the expected values of  $M$  in  $\vec{x}$ :

$$(\Delta M)_{\text{tot}}^2 = \langle(\Delta M)^2\rangle + (\Delta\langle M \rangle)^2. \quad (20)$$

This expression is used later on to calculate the mass dispersion of the simulations. At the beginning of the dynamical development, any scatter in BCG absolute magnitudes or masses is the sum of different kinds of model dispersion:

1. The statistical variation at constant model parameters within an ensemble, whereby one gets a convolution of two distributions: the stochastic variance at a constant vector of model parameters and
2. the variance caused by the distribution of clusters upon the model parameters.

Hence the observed relative mass dispersion is the upper limit of the statistical error.

In this context it is astonishing that there is definitely no correlation between  $M_{\text{BCG}}$  and richness (meaning the final galaxy number) in today's observed clusters (Sandage (1972); Postman & Lauer (1995)). But drawing galaxies from a distinct distribution (except from a  $\delta$ -function), there is always – within the bounds of resolution – such a dependence, so that

there inevitably has to be another process to explain the independence of  $M_{\text{BCG}}$  on  $N$ . The simulations try to answer the question whether mergers can account for such a behaviour. The observed scatter in absolute magnitudes is in any case an upper limit of the intrinsic BCG mass dispersion within any ensemble.

The dependence of the BCG absolute magnitudes on the scaling mass  $M_0$  is more complicated.  $M_0$  is positively correlated with  $M_{\text{BCG}}$  with high statistical significance. In order to eliminate any photometric calibration error as well as a global shift of the luminosity function, Trèvese, Cirimele, & Appodia (1996) compare  $M_{\text{BCG}} - M_{10}$  ( $M_{10}$  is the magnitude of the 10th brightest galaxy) with  $M_0 - M_{10}$ . They find, that both differences are negatively correlated.

#### 4. Results

Table 1 lists the input parameters of the simulation.

Here the two parameters  $R$  and  $N$  are allowed to vary independently (2) in the given interval while the pair  $(M_0; r_0)$  remains constant. Then, the mean relative velocity computed using the virial theorem adjusts automatically. Afterwards a new pair  $(M_0; r_0)$  is fixed from the variation interval, and  $N$  and  $R$  are varied again.  $M_0$  and  $r_0$  are not correlated.  $k$  is set to 1 or 10 (the probable value of present clusters).

The underlying idea is that there is a fixed value of  $M_0$  for all clusters in nature within narrow limits (corresponding to the fixed  $L_*$  in the Schechter distribution), that the mass-to-light ratio of all clusters is initially the same and that all galaxies of equal initial mass are of the same size, independent of cluster membership.

On the other hand, there are clusters of different size and variable richness in nature that enter the measurements of mass dispersion of the brightest cluster galaxies and are equally put together.

At the end of the simulation the following ensemble mean data are derived:

1. The mean relative velocity calculated from the virial theorem,
2. the number of galaxies at the end of the simulation,
3. the total number of encounters within the maximum impact parameter,
4. the number of constructive merger processes,



5. the number of destructive merger processes,
6. the number of destroyed galaxies without forming a remnant,
7. the number of merging events that lead to the formation of the BCG,
8. the BCG mass,
9. the BCG mass ensemble dispersion.

Except for the last two items giving the relative mass dispersion, the data serve as investigation of the model and are not connected to observations.

#### 4.1. The simulation with $M_0 = 5 \cdot 10^{11} M_\odot$ , $r_0 = 20\text{kpc}$ and $k = 1$

In the following, results of this parameter set are discussed in detail. Concerning other values of  $M_0$ ,  $r_0$  and  $k$  only occuring changes in contrast to this set are mentioned.

The choice of  $M_0 = 5 \cdot 10^{11} M_\odot$  means a moderate mass-to-light ratio of about  $\Upsilon_{galaxies} = 10$  of today's observed clusters, i.e. the absence of dark coronae, and  $k = 1$  means the initial absence of intergalactic matter.

The number of encounters of all galaxies is shown in Fig. 5. This total number of encounters increases within the bounds of parameter variation to  $10^6$  and corresponds essentially to Eq. 7, substituting the total development time  $T$  for  $\Delta t$ . Therefore the number of encounters is proportional to  $N^{5/2}$  and to  $R^{-7/2}$  and changes in the course of evolution only at small radii  $R$ , where the galaxy number decreases due to merger and destruction processes (cf. Fig. 10).

Figure 6 shows the mean BCG masses at the end of the simulation. They are located between about 30 and  $70 \cdot 10^{11} M_\odot$  and show a clear peak at small radii and small initial galaxy numbers.

In order to exclude the influence of the initial mass distribution in this histogram, the pure mass increase is shown in Fig. 7. Generally the BCG is growing in the course of development. The increase amounts to  $40 \cdot 10^{11} M_\odot$  at the peak which stands out even more clearly than in Fig. 6.

The main result of the simulation, i.e. the mean values of the BCG relative mass dispersion, is shown in Fig. 8. The dispersion is nearly constant at about thirty per cent and increases at the small clusters to a maximum of 57 %.

Table 1: Simulation parameters

Parameter	Value(s)	Remark
Ensemble size	$n = 100$	constant
Total time	$T = 10$ Gyr	constant
Char. mass	$M_0 \in \{5; 50\} \cdot 10^{11} M_\odot$	variable (1)
Char. radius	$r_0 \in \{20; 100\}$ kpc	variable (2)
$\Upsilon$ ratio	$k \in \{1; 10\}$	variable (1)
Cluster radius	$R \in [0.25; 3.00]$ à 0.25 Mpc	variable (2)
Richness	$N \in [100; 1000]$ à 100	variable (2)

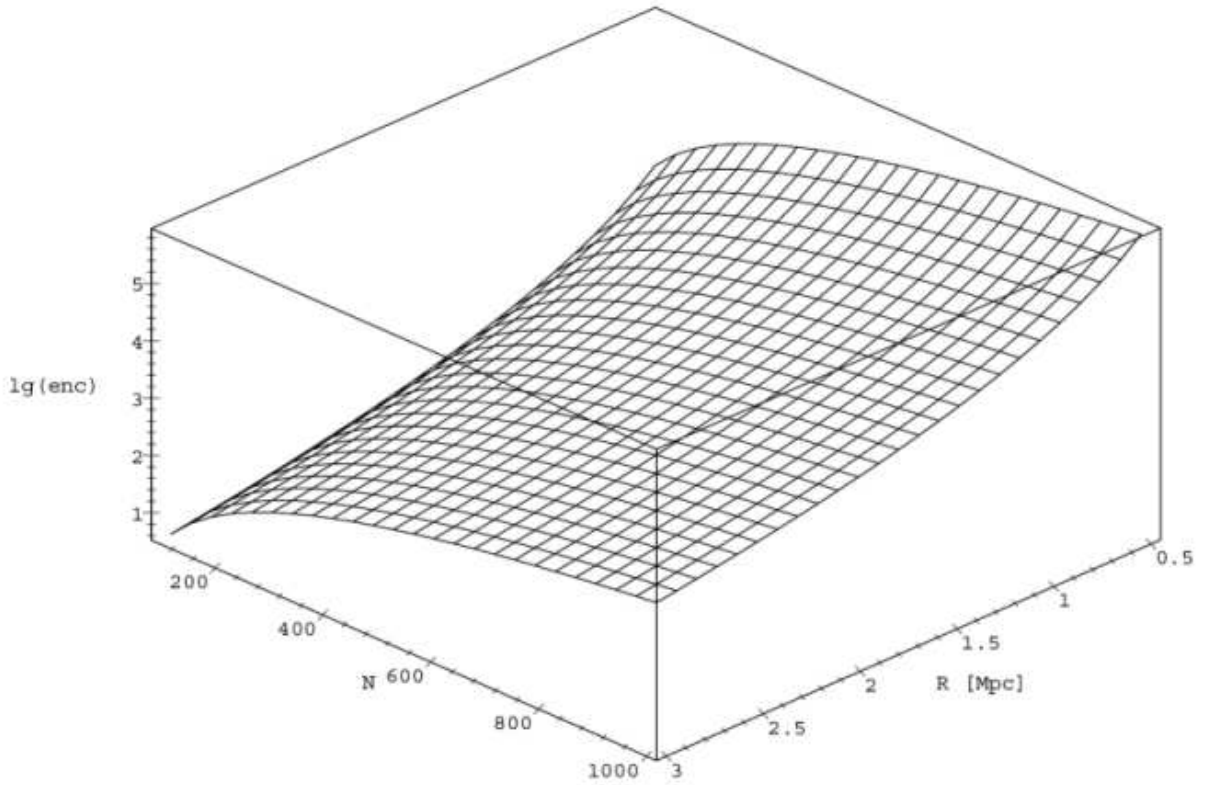


Fig. 5.— Logarithm of the total number  $p$  of encounters.

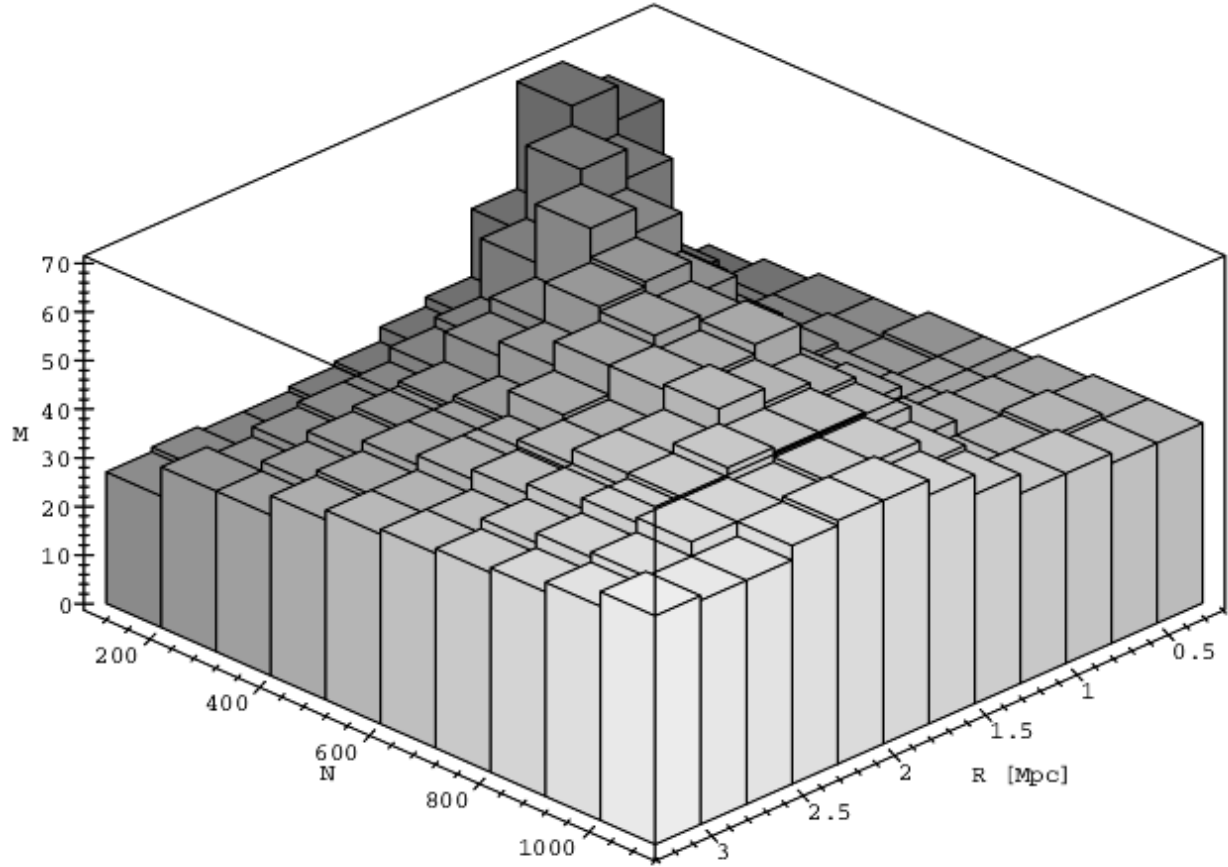


Fig. 6.— Mean values of BCG masses after the development.  $M = \langle M_{\text{BCG}} \rangle [10^{11} M_{\odot}]$ .

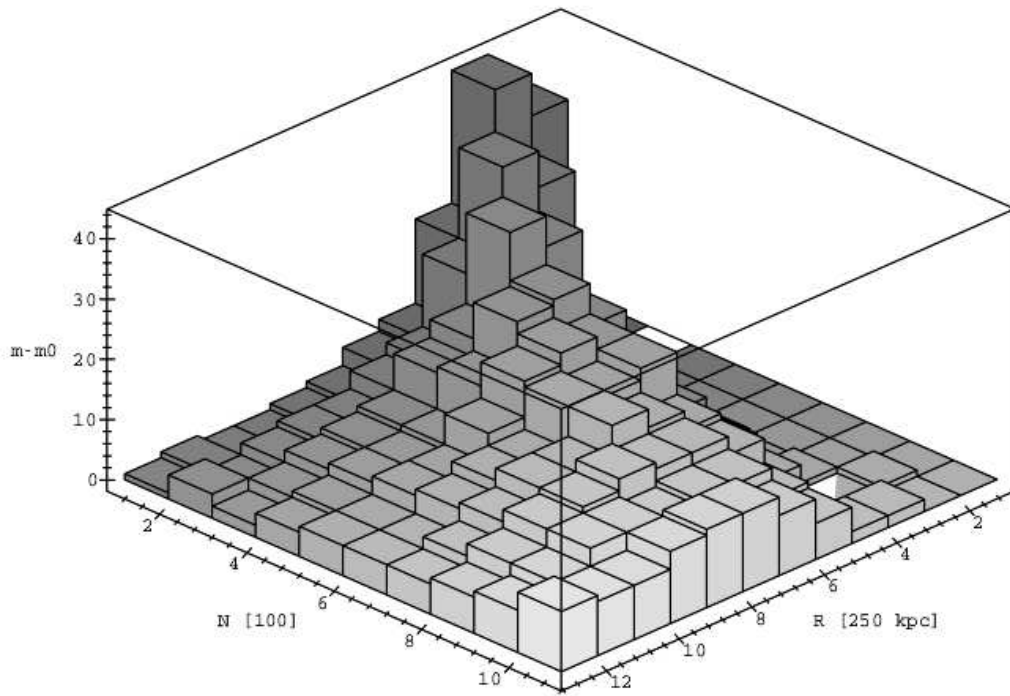


Fig. 7.— Mean values of BCG mass increase.  $M - M0 = \langle M_{\text{BCG,afterwards}} \rangle - \langle M_{\text{BCG,previously}} \rangle [10^{11} M_{\odot}]$ .

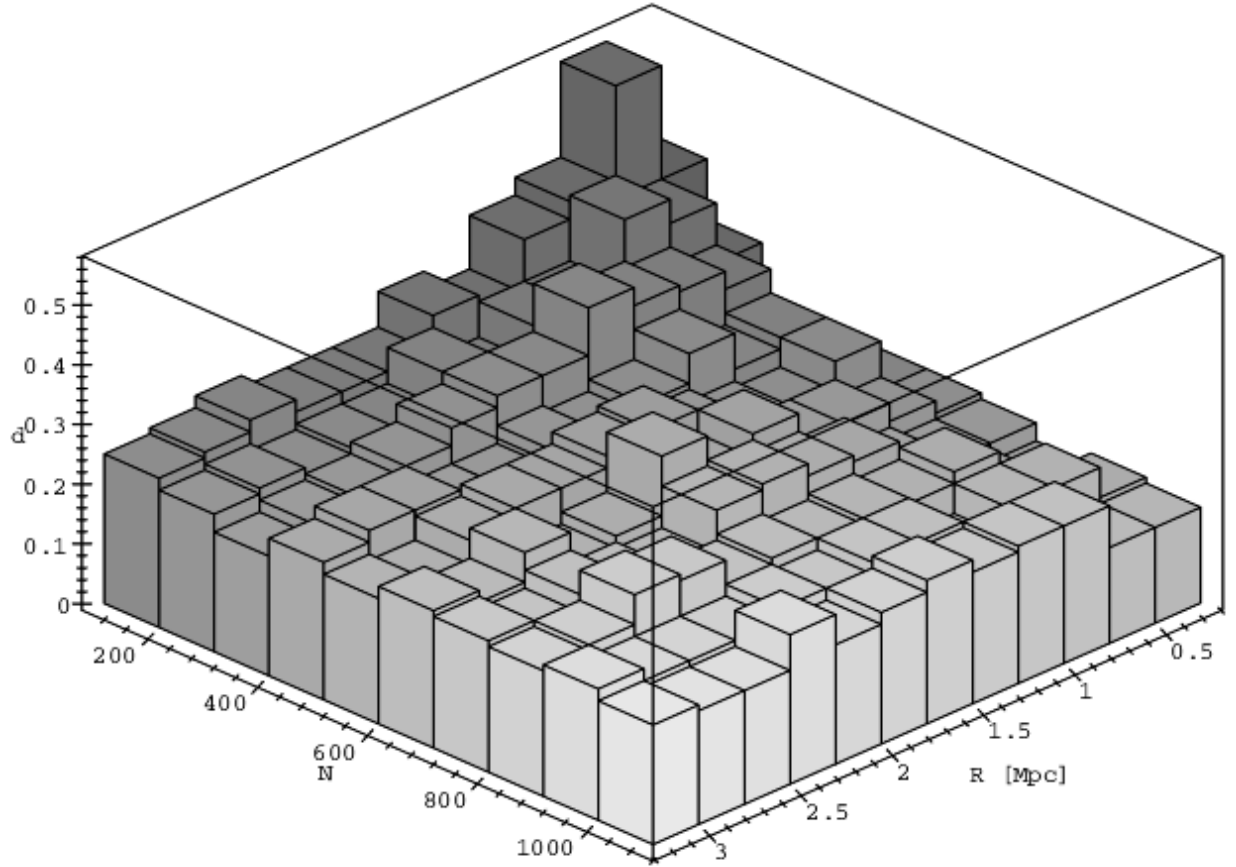


Fig. 8.— Mean values of BCG mass dispersion after the simulation.  $d = \langle \sigma_{\text{BCG}} \rangle / \langle M_{\text{BCG}} \rangle$ .

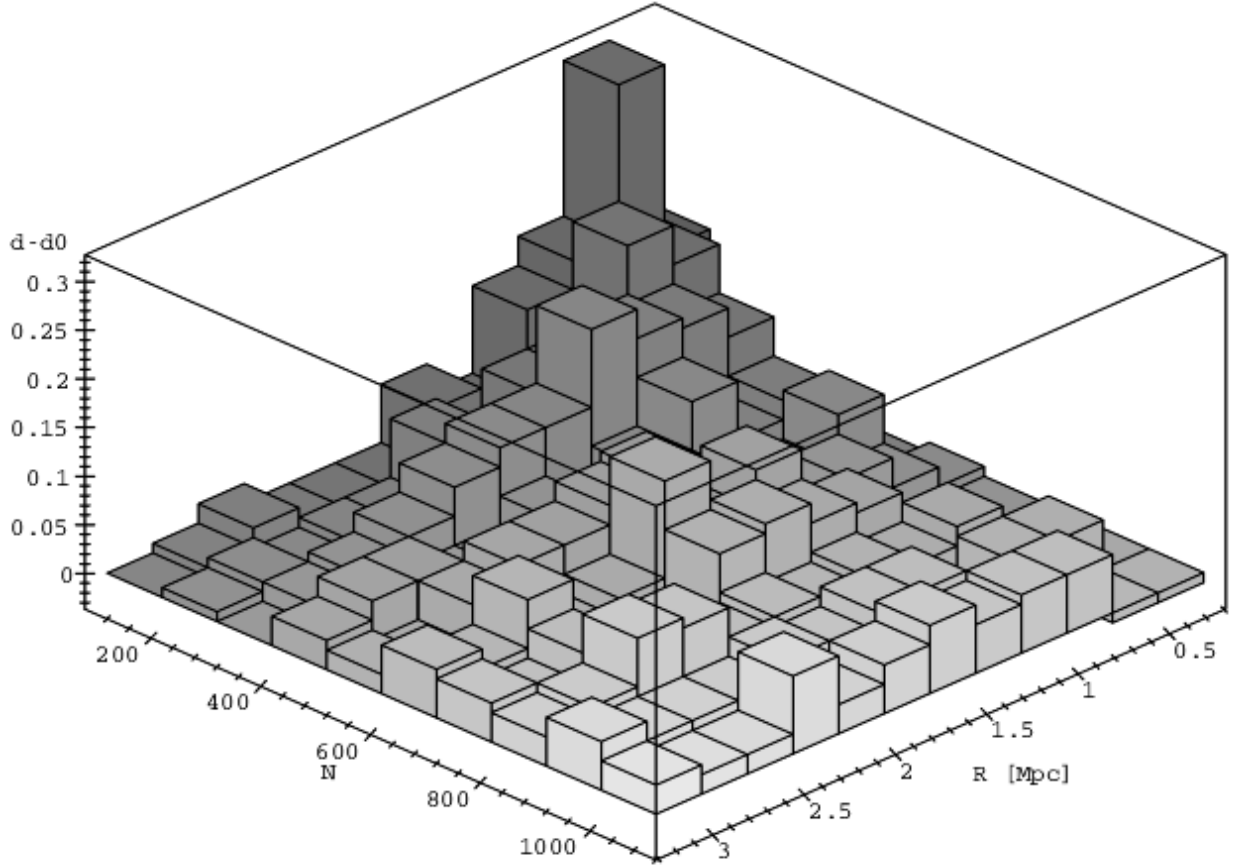


Fig. 9.— Mean values of the increase of BCG mass dispersion.  $d - d0 = \langle \sigma_{\text{BCG,afterwards}} \rangle / \langle M_{\text{BCG,afterwards}} \rangle - \langle \sigma_{\text{BCG,previously}} \rangle / \langle M_{\text{BCG,previously}} \rangle$ .

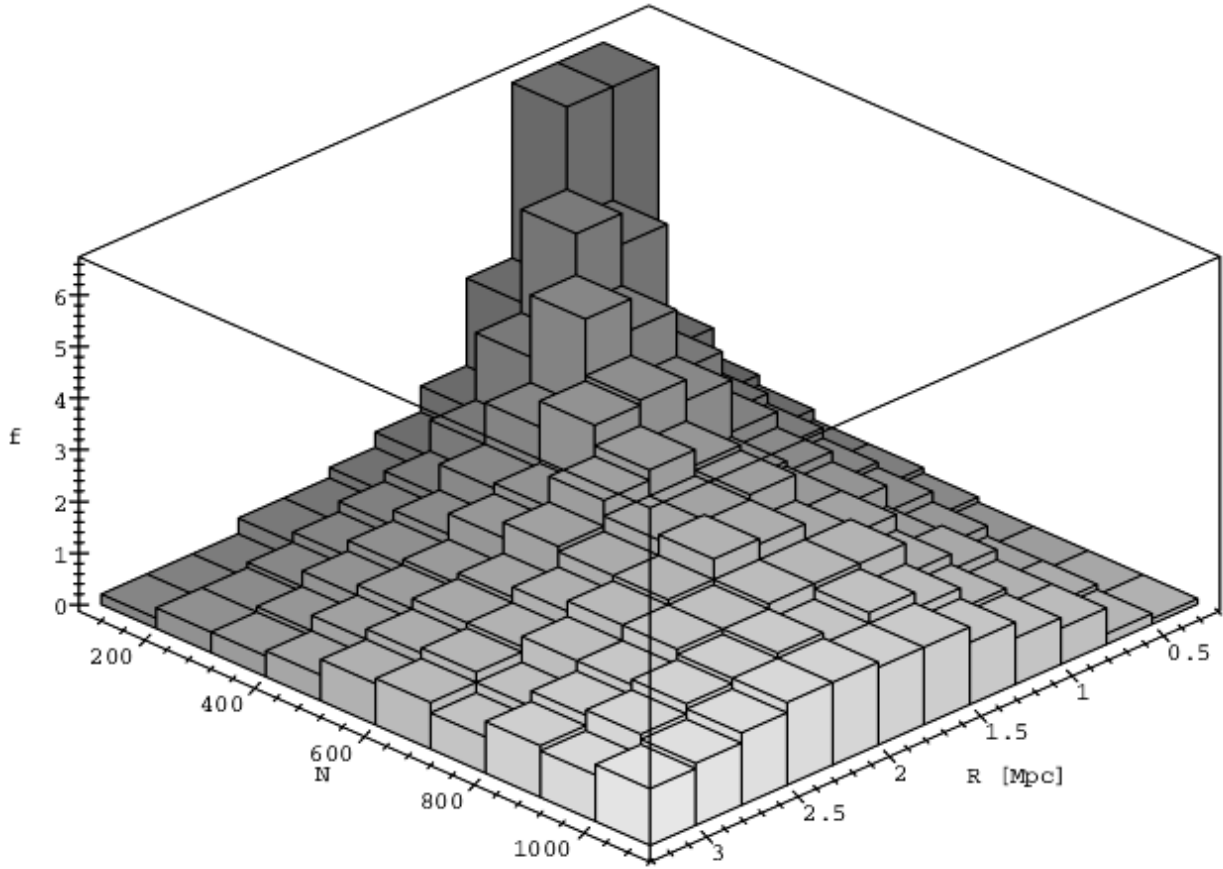


Fig. 10.— Mean number of mergers leading to the BCG formation.

In order to investigate the increase in mass dispersion as in Fig. 7 and to exclude the influence of the initial distribution, the relative mass distribution after the simulation is subtracted by the relative dispersion before the simulation in Fig. 9. As in Fig. 7, the peak stands out more clearly against the stochastic noise.

To answer the question how many mergers are necessary to form the BCG this parameter  $f$  is shown in Fig 10. The maximum value lies at about six mergers and decreases steeply from there to a value of about one.

Not only merger events but also destructions of galaxies are part of cluster development. Figure 11 shows how many galaxies are left at the end of the simulation. Here a clear trend is recognizable: the percentage of destroyed or merged galaxies increases considerably with decreasing cluster radius. In the case of rapid evolution the number of galaxies may decrease down to twenty per cent of the original value.

The difference between Fig. 11 and Fig. 13 provides roughly for the number of galaxies destroyed in encounters (Fig. 12). It turns out that the biggest fraction of galaxies is destroyed when the energy transfer is less than the sum of binding energies of the 2 galaxies. The percentage of disrupted galaxies is always less than 65 per cent and decreases with increasing radius. At small radii the fraction of destroyed galaxies is roughly independent of the initial galaxy number, but increases with galaxy number at increasing radii.

Finally, to address the question about the fate of the remaining galaxies, the number of all the merger events of all galaxies is divided by the final galaxy number in Fig. 13. The parameter  $t$  in this diagram denotes the percentage of those galaxies that are involved in a merger event. In the same way  $t$  is a measure of the frequency describing how often a galaxy has been involved in a merger event averaged over all cluster galaxies. In the peak vicinity every galaxy has experienced one merger on the average.  $t$  sharply decreases with increasing  $N$  and  $R$ .

#### 4.2. The simulation with $M_0 = 5 \cdot 10^{11} M_\odot$ , $r_0 = 20\text{kpc}$ and $k = 10$

The choice of  $M_0$  and  $r_0$  corresponds to the choice in Sect. 4.1,  $k = 10$  corresponds (at  $M_0 = 5 \cdot 10^{11} M_\odot$ ) roughly to the maximum value of the present fraction of intergalactic dark matter in galaxy clusters.

The mass distribution of single galaxies corresponds exactly to the one of Sect. 4.1, but because of the addition of intergalactic matter the virial velocity is increased by the factor  $\sqrt{10}$  according to Eq. 6. This is why the number of encounters is about this factor higher



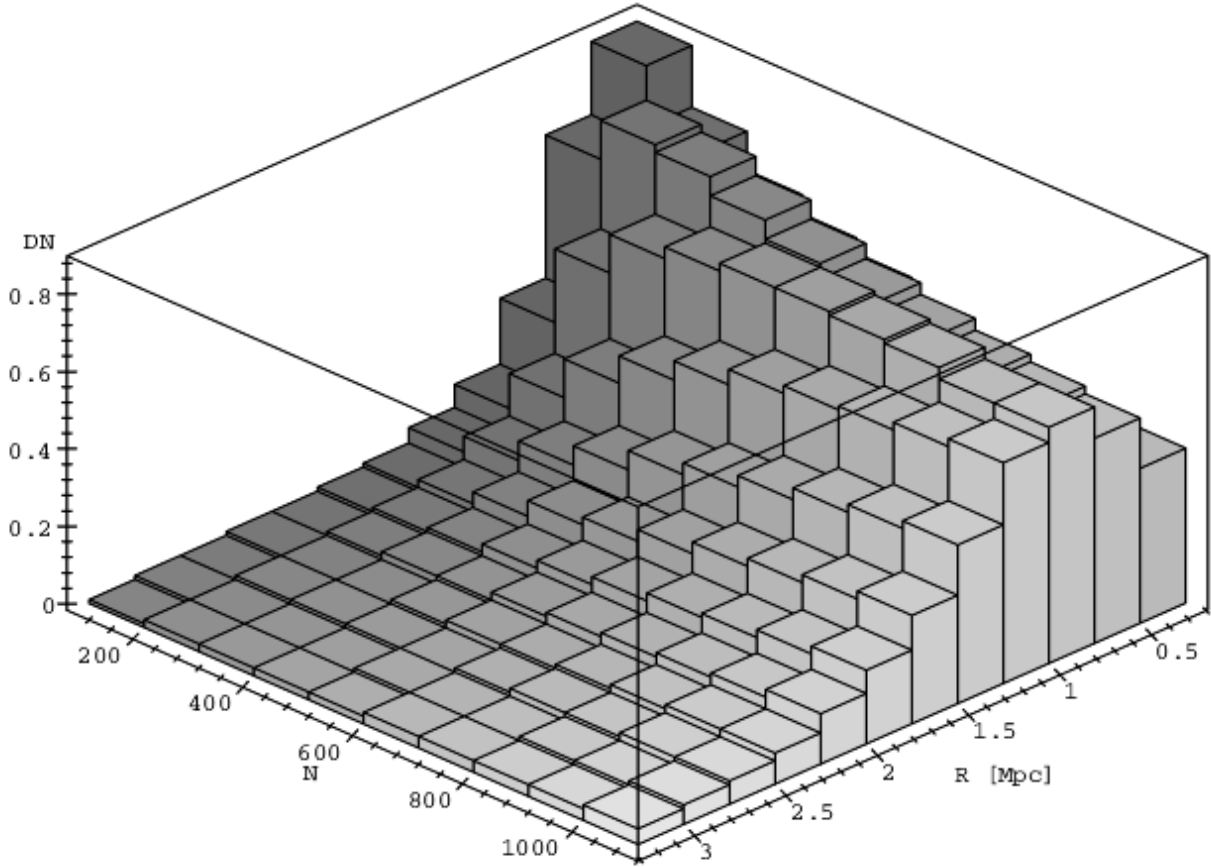


Fig. 11.— Mean number of destroyed/merged galaxies per initial galaxy number after development.

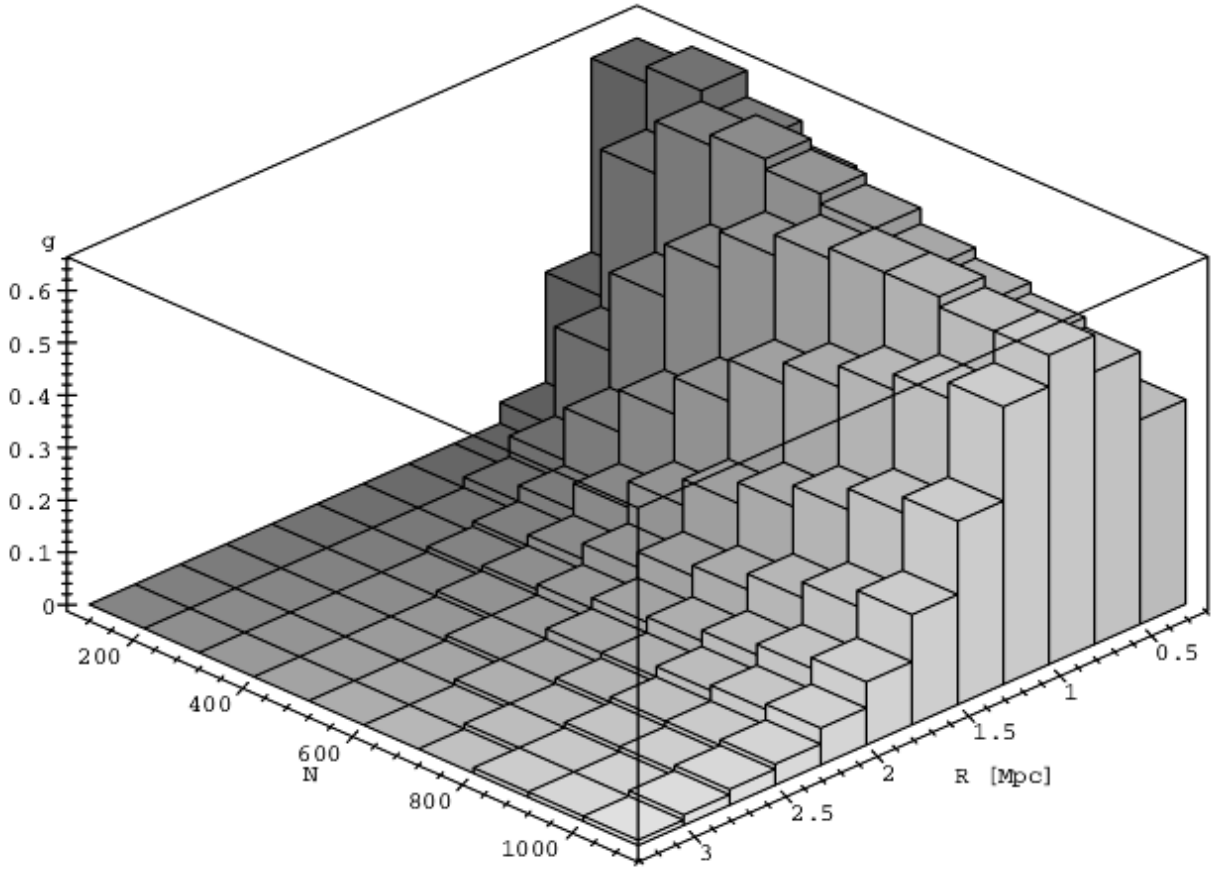


Fig. 12.— Percentage of destroyed galaxies.

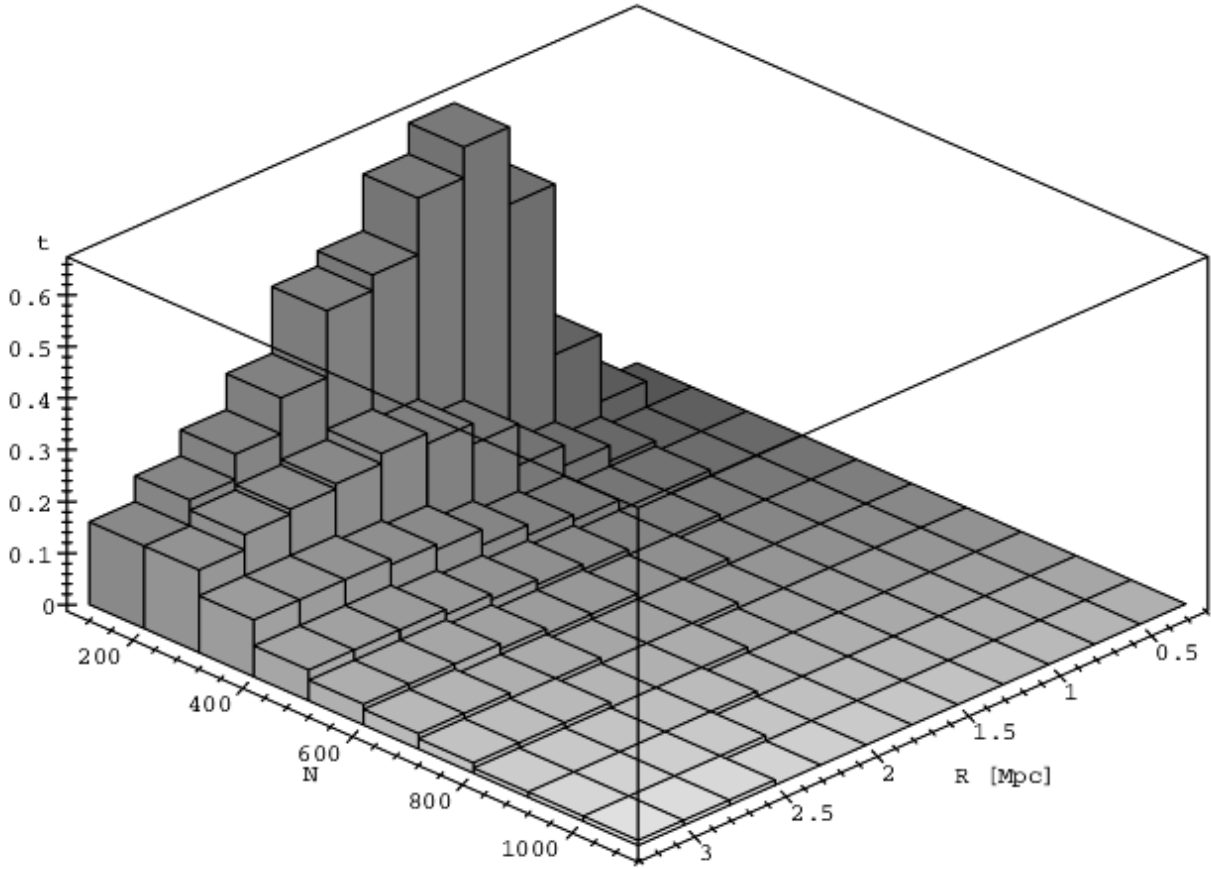


Fig. 13.— Mean number of merger events per final galaxy number.

in comparison with Fig. 5. The high spatial velocity-dispersions a little above the diagonal of more than 2400 km/s are not observed in reality; therefore this part of the simulation is excluded in the following discussion.

The final galaxy numbers drop to values of significantly less than hundred per cent at small radii. The qualitative behaviour follows the one of Fig. 11, but the maximum is, however, clearer marked at small radii and galaxy numbers, and about half as many galaxies less have been destroyed at a fixed pair  $(R, N)$  compared with Sect. 4.1. The dominant development process here is not merging but destruction of encountering galaxies. The mean mass distribution of BCGs after the simulation has not changed much: The initial mass distribution can easily be recognized. Deviations in comparison to the initial distribution arise in about half of the cases, these deviations are about  $\pm 1 \cdot 10^{11} M_{\odot}$  for each half.

Only little signs of evolution are present in the BCG mass dispersion after the simulation: The initial mass scatter is still present. The relative dispersion does not exceed a value of 25 per cent. The trend of the initial distribution having smaller spreads with increasing galaxy numbers still exists. Just as for the mean mass values there is an irregular change in the scatter of 1–2% compared with the initial scatter.

### 4.3. The simulation with $M_0 = 50 \cdot 10^{11} M_{\odot}$ , $r_0 = 100 \text{ kpc}$ and $k = 1$

The total mass of the galaxy cluster is the same here as in Sect. 4.2, the galaxies however are ten times more massive.  $k = 1$  means the initial absence of intergalactic matter as in Sect. 4.1. The dark matter is now hidden in individual halos instead of spread throughout the intergalactic medium. Therefore more extended galaxies with a characteristic radius of  $r_0 = 100 \text{ kpc}$  are chosen at this parameter set.

Figure 14 shows the BCG mass mean values after the development. In comparison with Fig. 6 the shift of the maximum toward smaller galaxy numbers but significantly greater cluster radii is striking.

Figure 15 makes it clear that the relative mass dispersion remains always below forty per cent and even decreases significantly going to greater galaxy numbers, particularly at this set of parameters.

Fig. 16 shows that the number of mergers leading to the formation of the BCG is non-zero for a wider range of parameters  $N$  and  $R$ . The maximum mean number of mergers is four as in Sect. 4.1.

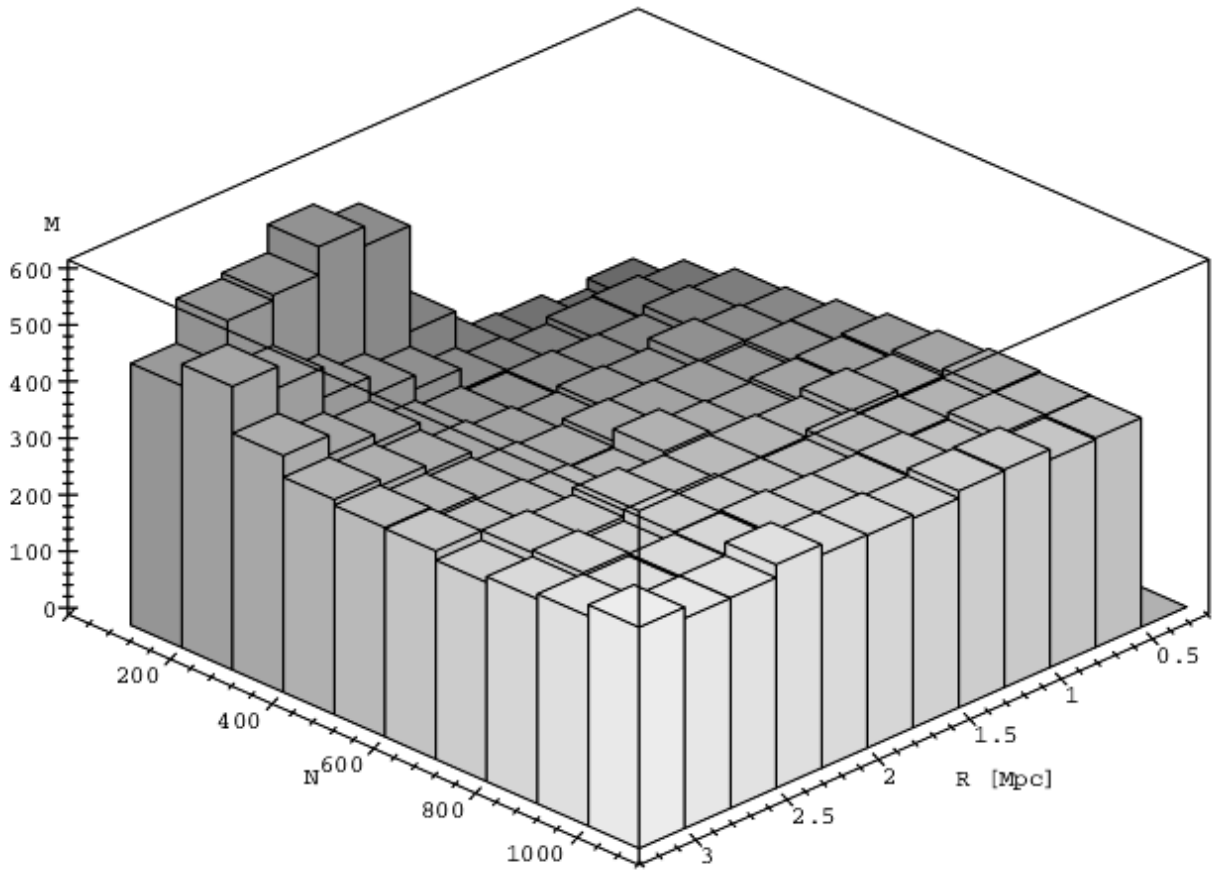


Fig. 14.— Same as Fig. 6, but now for model 4.3.

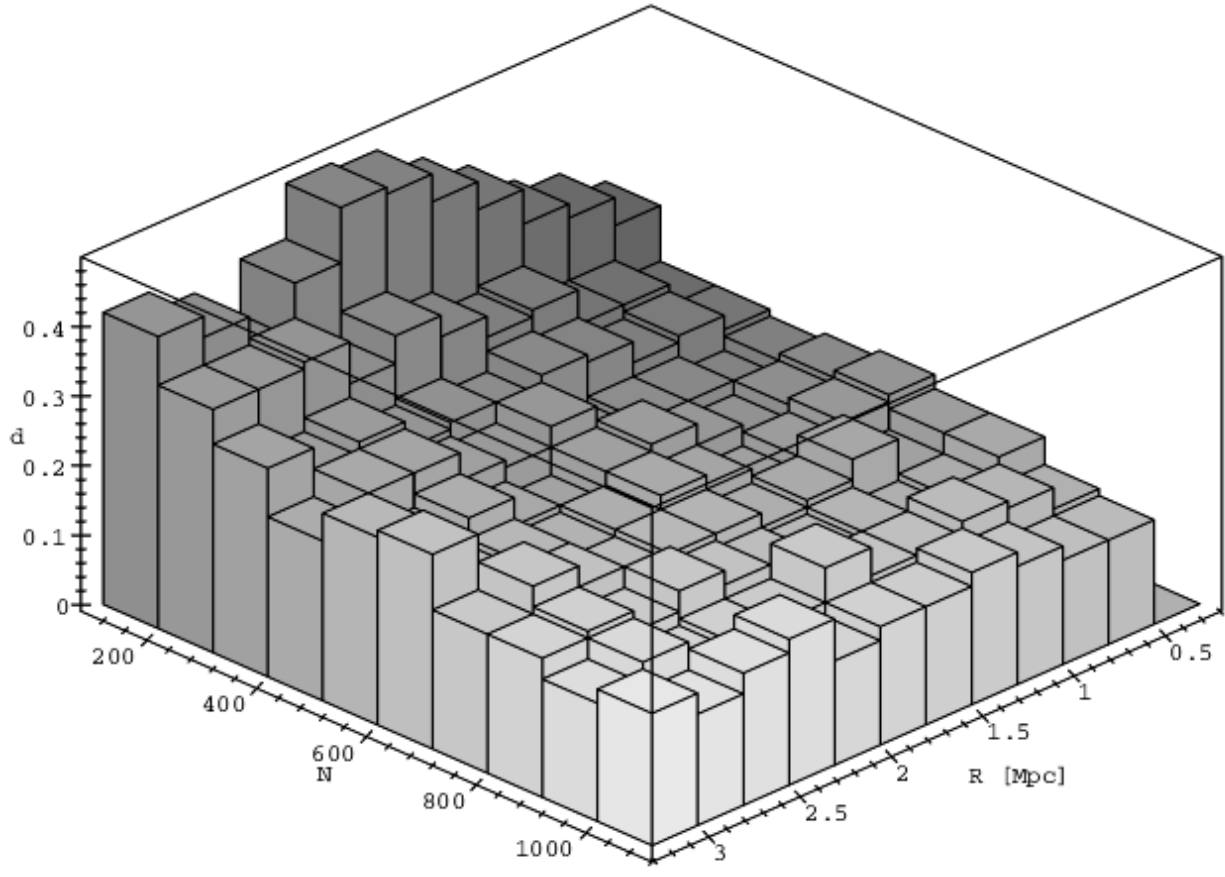


Fig. 15.— Same as Fig. 8, now for model 4.3.

At smaller galaxy numbers the percentage of those galaxies that have been involved in merger processes increases up to sixty per cent (Fig. 18), cf. also Fig. 13. From a galaxy number of about four hundred onwards there are practically no merger events to be noted.

## 5. Discussion

There are two processes with opposite effects which rule the evolution of the model: On the one hand the number of encounters decreases with increasing cluster radius at fixed galaxy number (cf. Fig. 5). On the other hand the virial velocity increases with increasing total cluster mass by increasing richness at fixed cluster radius. Although the number of encounters rises with velocity, the equations of energy transfer (Eqs. 11 and 12) depend on  $v^{-2}$ , and the kinetic energy term of the relative motion depends on  $v^2$ . So high energy transfers are only effective for mergers at low velocities. Taking both effects together, only compact groups evolve noticeably in contrast to clusters. The number of encounters  $g$  of a single galaxy for the total development time can be estimated to

$$g = \frac{N - 1}{4\pi R^3/3} \pi B^2 v T \quad (21)$$

if richness does not change dramatically. The merger probability can be estimated in the same way: let  $b_m$  be the impact parameter so that the merger criterion is fulfilled within its enclosed area:

$$b_m = \sqrt{\frac{32}{3}} \frac{\sqrt{Gm_0 r_0}}{v}. \quad (22)$$

Then the fraction of merger events (caused by the stochastic choice of impact parameters) is  $b_m^2/B^2$ . This fraction multiplied by the number of encounters then reveals the number of merger events  $V$  of one galaxy (e.g. the BCG):

$$V = 8f^{-1} r_0 T \sqrt{Gm_0} \cdot \sqrt{\frac{N}{R^5}} \quad (23)$$

So the number  $t$  of mergers depends strongly on the cluster radius and decreases with increasing  $R$  (cf. Fig. 11). On the other hand  $t$  increases proportional to the square root of the initial number of galaxies (assumed that it remains nearly constant, e.g. Fig. 11 at  $R = 0.75$  Mpc and higher). The boost of constructive (remnant forming) or destructive encounters can thus be explained, but not the merger boost at low galaxy numbers. Furthermore it has to be taken into account whether the remnant remains bound. That leads to

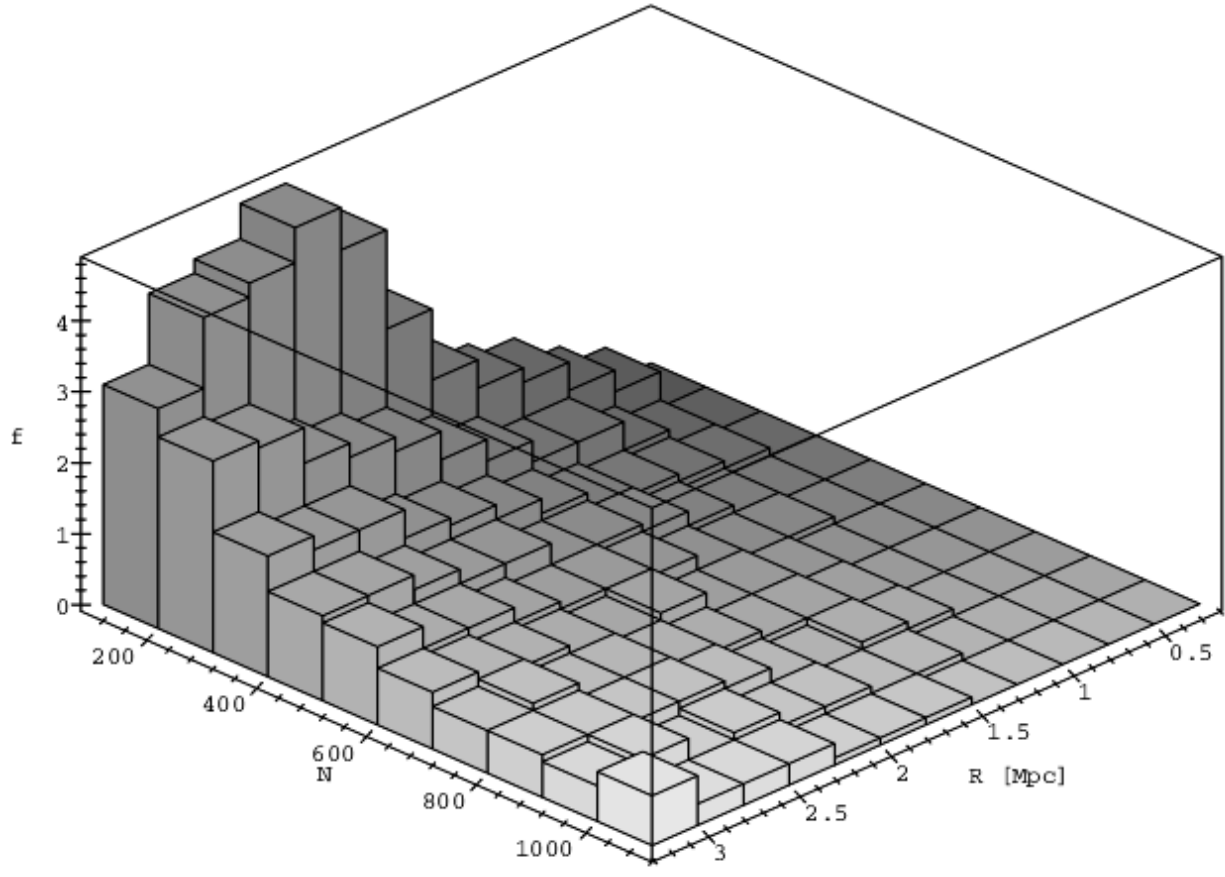


Fig. 16.— Same as Fig.10, now for model 4.3.



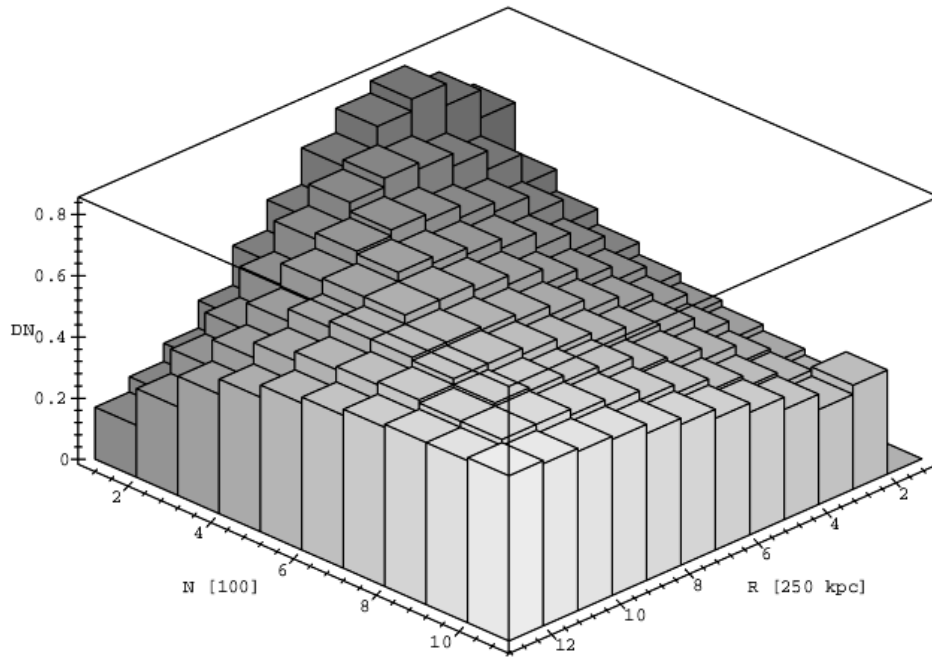


Fig. 17.— Same as Fig.11, now for model 4.3.

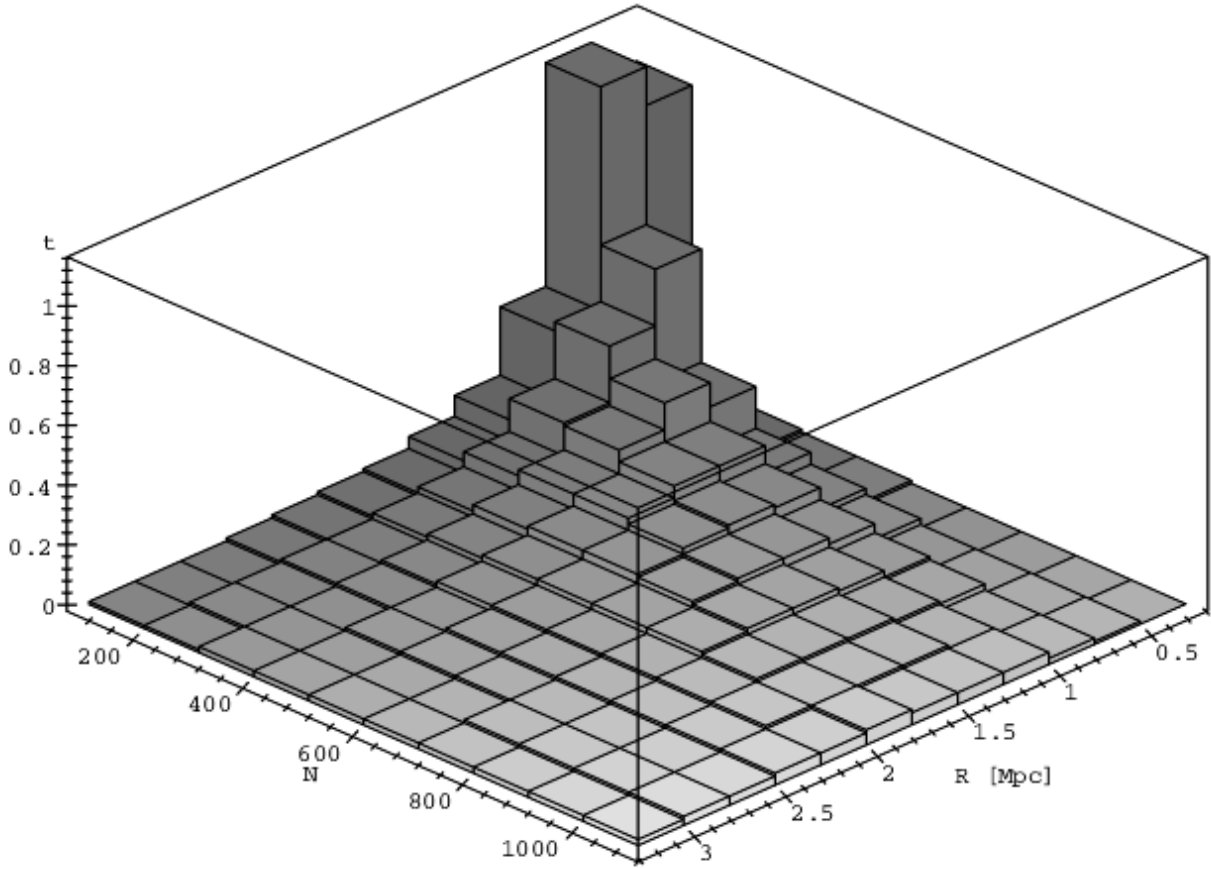


Fig. 18.— Same as Fig.13, now for model 4.3.

$$\frac{3\pi\beta}{8r_0f^2} \cdot \frac{R}{N} > 1. \quad (24)$$

The remnant has a chance to survive only at high cluster radii and small galaxy numbers. Together with the merger criterion this leads to the occurring maximum development at small cluster radii and small numbers of galaxies (Figs. 7, 10, 13): Small radii are necessary to form remnants, and their binding energies are negative only at small galaxy numbers.

These estimates expressed in simple formulae (Eqs. 21-23) are possible because our simulation show that there is no agravating change of the initial mass distribution.

The simulation computations of Sect. 4.3 show a merger behaviour of all galaxies and especially of those forming the BCG comparable to Sect. 4.1. A higher galaxy mass has a positive effect on the number of mergers because the mean energy transfer rises with the third power of the characteristic mass, whereas the kinetic energy of the relative motion still rises linearly. On the other side a higher cluster mass in Sect. 4.3 in contrast to Sect. 4.1 causes the virial velocity to increase, suppressing energy transfer such as in Sect. 4.2.

Interpreting simulation 4.2 to represent cluster states further evolved in time compared with simulation 4.1 as the mass of the intergalactic medium increases due to tidal stripping (Merritt (1984)), a picture of cluster evolution is formed: In the early phases of cluster evolution merger processes dominate the development of mass spectrum and BCG, then paling into insignificance as time goes by (cf. Albinger (1995)). Comparing both simulations it should be noted that the cluster mass is the same in simulation 4.2 at  $N = 100$  and simulation 4.1 at  $N = 1000$ . An increase of the mass fraction of intergalactic matter leads to a drastic decrease in the merger rate at equal galaxy mass distributions, because the mean kinetic energy controlled by the virial theorem (Eq. 6) outgrows the expected energy transfers in Eq. 13, so that mergers become improbable. The amount of galaxy binding energy is not influenced by a variation of  $k$ , and so a (less steep) decrease in galaxy destructions is expected on the basis of Eq. 13 as shown by the simulations.

A closer consideration of Fig. 7 together with Fig. 10, dividing the mean increase of BCG mass by the mean number of mergers leading to the BCG formation, shows that the brightest galaxy must have been built by mergers of galaxies of uniform mass  $M_0$  independent of general conditions of the cluster. This is in accordance with the observation results of Hoessel (1980).

Figure 13 gives information about the number of constructive mergers per final galaxy number, i.e. the fraction of galaxies that merged with other galaxies during the simulation. This percentage is equivalent to the averaged number of mergers a galaxy has undergone.

This fraction rises going from high to small cluster radii and amounts to between some and about hundred per cent. Toomre (Shu (1982)) speculated that perhaps all elliptical cluster galaxies have been built by mergers. From the fraction of galaxies that are presently involved in gravitational interactions and the probable life time of this passing phenomena he calculated that merging of spiral galaxies happens for a fraction of about ten per cent of all cluster galaxies, in good agreement with the results of this work. The fact that especially rich compact clusters which are assumed to be dynamical older systems than spiral rich ones have a significantly larger fraction of elliptical galaxies (up to 35 per cent in the Coma cluster (cf. Oemler (1974))) may have multiple reasons. First a comparison of the simulations in Sects. 4.1 and 4.2 shows that mergers grind to a halt at rising fraction of intergalactic matter, as the fraction of prospective interacting galaxies decreases at constant total cluster mass due to mergers and destructions. Hence the merger rate is higher in a cluster of earlier state of development (corresponding to irregular spiral rich clusters) than in the final state of compact clusters. So the fraction of elliptical galaxies in Toomre’s estimation has to be corrected upwards. Secondly elliptical galaxies may be a result of disturbances caused by nearby passages without merging that would lead to its rise to the presently observed value.

The percentage of galaxies destroyed in encounters (Fig. 12) yields an estimate of the dark matter fraction in clusters provided by destroyed galaxies. This fraction amounts up to 60 per cent corresponding to a ratio of cluster mass and total galaxy mass of  $k = 2.5$ .

Further simulations with the presented model were carried out using other sets of parameters without leading to different results than discussed in this work. Particularly an increase in galaxy numbers beyond a value of 1000 does not change anything, because the evolution of any model with scales comparable to clusters takes an imperceptible course at high galaxy numbers.

## 6. Conclusions

There is a common result from all simulations of Sect. 4: the cluster evolution is tightly related to the evolution of the brightest galaxy of this cluster. Only at small galaxy numbers and simultaneously at small cluster radii the dynamical development due to the model described in Sect.2 plays a noticeable role (cf. e.g. Fig. 10). At the same time increasing merger action is a concomitant of increasing destruction of galaxies. So, in the parameter range of rapid evolution, the number of galaxies depleted such that the evolved small cluster looks like a compact group rather than an Abell cluster. Nevertheless merging is always the dominant process (at least for the most massive galaxies). For clusters of presently observed richness and their most luminous member (being the comparative value to our simulation)

the dynamical development of the mass spectrum and of correlated quantities as the BCG mass causes only little changes with respect to the initial conditions.

Considering Fig. 6 and Fig. 8 the steadiness of BCG masses and their ensemble dispersion attract attention (irrespective of compact groups). This approximate independence of masses on cluster radius is observed in reality, and there are two causes that balance each other: At the beginning of the simulation the BCG masses are small and rise with increasing richness. In the course of evolution mergers take place preferentially at low galaxy numbers resulting in a relatively constant BCG mass level after the development in dependence of the parameters  $R$  and  $N$ . Taking into account an additional correlation between cluster radius and richness (e.g. Oemler (1974)) the BCG mass steadiness would turn out almost clearer, just as their dispersion would be narrower than stated in this work because of the restriction in parameter space.

Why does the BCG mass scatter remain significantly narrow even at the end of cluster development? First of all the number of mergers is relatively small for the mentioned reasons (between one and six merger events depending on the parameter set), and secondly the identity of a galaxy to be BCG is fixed only when the cluster development is complete. So, not the mass dispersion of a distinct galaxy fixed before the starting development is investigated, but the mass dispersion of a galaxy that is a posteriori identified to be the most massive one. Therefore the BCG mass dispersion turns out to be smaller than in the case of any individual galaxy chosen at the beginning of the simulation and following its evolution.

I thank Prof. Dr. R. Wielen and Prof. Dr. B. Fuchs for stimulating discussions and Dr. S. Frink for help in the preparation of this work for publication.

## REFERENCES

- Aguilar, L.A., White, S.D.M., 1985, ApJ, 295, 374
- Albinger, C., 1995, degree dissertation at Ruprecht-Karls-Universität Heidelberg, Germany
- Batcheldor, D., Marconi, A., Merritt, D., Axon, D.J., 2007, ApJ, 663, L85
- Bird, C.M., 1994, ApJ, 107, 1637
- Bode, P.W., Berrington, R.C., Cohn, H.N., Lugger, P.M., 1994, ApJ, 433, 479
- Dressler, A., 1978, ApJ, 222, 23

- Dubinski, J., 1998, *ApJ*, 502, 141
- Funato, Y., Makino, J., Ebisuzaki, T., 1993, *PASJ*, 45, 289
- Garijo, A., Athanassoula, E., García-Gómez, C., 1997, *AA*, 327, 930
- Geller, M.J., Peebles, P.J.E., 1976, *ApJ*, 206, 939
- Hoessel, J.G., 1980, *ApJ*, 241, 493
- Hoessel, J.G., Gunn, J.E., Thuan, T.X., 1980, *ApJ*, 241, 486
- Humason, M.L., Mayall, N.U., Sandage, A.R., 1956, *AJ*, 61, 97
- Jagemann, Th., 1997, degree dissertation at Ruprecht-Karls-Universität Heidelberg, Germany
- Krivitsky, D.S., Kontorovich, V.M., 1997, *A&A*, 327, 921
- Lauer, T.R., 1985, *ApJ*, 292, 104
- von der Linden, A., Best, P.N., Kauffmann, G., White, S.D.M., 2007, *MNRAS*, accepted for publication
- De Lucia, G., Springel, V., White, S.D.M., Croton, D., Kauffmann, G., 2006, *MNRAS*, 366, 499
- Merritt, D., 1983, *ApJ*, 264, 24
- Merritt, D., 1984, *ApJ*, 276, 26
- Merritt, D., 1985, *ApJ*, 289, 18
- Motl, M.M., Burns, J.O., Loken, C., Normann, M.L., Bryan, G., 2004, *ApJ*, 606, 635
- Oemler, Aug.Jr., 1974, *ApJ* 194, 1
- Ostriker, J.P., Hausman, M.A., 1977, *ApJL*, 217, 125
- Peres, C.B., Fabian, A.C., Edge, A.C., Allen, S.W., Johnstone, R.M., White, D.A., 1998, *MNRAS*, 298, 416
- Postman, M., Lauer, T.R., 1995, *ApJ*, 440, 28
- Sandage, A., 1972, *ApJ*, 178, 1

Schechter, P., 1976, ApJ, 203, 297

Schechter, P.L., Peebles, P.J.E., 1976, ApJ, 209, 670

Shu, F.H., 1982, The physical universe, University science books

Spitzer, L., 1958, ApJ, 127, 17

Springel, V., White, S.D.M., Tormen, G., Kauffmann, G., 2001, MNRAS, 328, 726

Springel, V., et al., 2005, Nature, 435, 629

Trèvese, D., Cirimele, G., Appodia, B., 1996, A&A, 315, 365